nadium(IV) complex has been found. Hydroxamate and catecholate ligands are unique to date in being able to break the strong V=O vanadyl bond in an aqueous environment.

Acknowledgment. This research was supported by NIH Grant AI 11744.

Registry No. $(VO(OCH_3)L)_2$ (n = 3), 123264-09-5; $(VO(OC_2H_5)L)_2$ (n = 3), 123264-10-8; $(VO(OCH_3)L)_2$ (n = 5), 123264-11-9; $(VO(OC_2H_5)L)_2$ (n = 5), 123264-12-0; $VO(OCH_3)L$ (n = 10), 123264-13-1; $VOCl(bz)_2$, 123264-15-3; $(VO(OiPr)L)_2$ (n = 5), 123264-16-4; $VO(acac)_2$, 3153-26-2; $VO(RA)(OCH_3)$, 123264-18-6; $VO(RA)\cdot H_2O$, 123264-19-7; $[V_2(RA)_3]^{2+}$, 123264-17-5; oxovanadium(IV) sulfate, 27774-13-6.

Supplementary Material Available: Figures S1 and S2, showing vis/UV spectra of vanadium(IV/V) rhodotorulate complexes from spectroelectrochemical experiments and vis/UV spectra of a vanadium(IV) rhodotorulate complex in solution upon exposure to air, and Tables S1, S4, and S5, listing crystallographic summary data and anisotropic thermal parameters for $VOCl(bz)_2$ and $[VO(OiPr)L]_2$ (n = 5) (6 pages); Tables S2 and S3, listing calculated and observed structure factors for $VOCl(bz)_2$ and $[VO(OiPr)L]_2$ (n = 5) (39 pages). Ordering information is given on any current masthead page.

Contribution from the Departments of Chemistry, University of Missouri—Rolla, Rolla, Missouri 65401, and Abilene Christian University, Abilene, Texas 79699, Nuclear Physics Division, Atomic Energy Research Establishment, Harwell, Didcot OX11 0RA, England, and Institut de Physique, Universite de Liege, B-4000 Sart Tilman, Belgium

Study of the High-Temperature Spin-State Crossover in the Iron(II) Pyrazolylborate Complex $Fe[HB(pz)_3]_2$

Fernande Grandjean, Gary J. Long,* Bennett B. Hutchinson,* LaNelle Ohlhausen, Paul Neill, and J. David Holcomb

Received January 6, 1989

A study of the infrared and Mössbauer spectra and magnetic properties of $Fe[HB(pz)_3]_2$ indicate that this nominally low-spin iron(II) compound undergoes a spin-state crossover to the high-spin state accompanied by a crystallographic phase change at about 400 K. The crystallographic phase transition shatters the crystals and leads to a large hysteresis in the magnetic moment upon cooling from 460 to about 250 K. The analyses of the Mössbauer spectra, obtained as a function of temperature during both heating and cooling, indicate the presence of spin-state relaxation on the Mössbauer time scale of 10^{-8} s. The activation energy for this relaxation process is 7300 cm^{-1} for freshly sublimed $Fe[HB(pz)_3]_2$ and 1760 cm^{-1} after the crystals have undergone the phase transition. Both the magnetic moments and Mössbauer spectra indicate that between 295 and 430 K the ground state of $Fe[HB(pz)_3]_2$ has a temperature-dependent population of both the high-spin and low-spin electronic configurations. The optical absorption spectrum provides further support for the spin-state crossover and DSC and volume expansion studies indicate the presence of the phase transition at the spin-crossover. Analysis of the far-infrared spectrum utilizing $^{54}Fe/^{57}Fe$ substitution at both room and high temperatures allows unambiguous assignment of the Fe–N stretching bands both in high-spin and low-spin forms. The low-spin Fe–N stretching bands appear at 459, 434.5, and 399.5 cm^{-1}, whereas upon heating the high-spin Fe-N stretching bands appear at 257.5 and 223 cm^{-1}. Measurement of the area of these bands as the temperature is increased reflects the change in the population of the low-spin and high-spin states.

Introduction

In 1931 Cambi and co-workers found an anomalous, temperature-dependent, magnetic behavior for several Fe(dialkyldithiocarbamate)$_3$ complexes.[1] Their investigation revealed a behavior which they attributed to a rearrangement of the electrons in the d orbitals as the temperature was decreased below room temperature. Twenty-five years later, Maki[2] and Ballhausen[3] applied crystal field theory to these and similar compounds, and attributed the magnetic behavior to a change from a high-spin, weak-field electronic configuration to a low-spin, strong-field configuration. Now transition-metal complexes with a variety of metals, oxidation states, and ligands, have been observed to change their spin-state and exhibit spin-crossover phenomena. First-row transition-metal complexes with $3d^4$ to $3d^7$ electronic configurations have been found to change between a high-spin and a low-spin configuration,[4] but iron complexes are the most abundant as indicated in various reviews.[5-9] The spin-crossover in these complexes may occur with changes in temperature, pressure,[10-12] and coordination number and with exposure to light.[13,14]

Additional interest in these compounds has been created by the recognition that, in some biologically significant molecules, spin-state change is an important part of their reaction mechanism.[15-17]

The tris(1-pyrazolyl)borate ligand, $HB(pz)_3^-$, and its methyl-substituted derivatives produce a ligand field in which iron(II) compounds may form either the high-spin or low-spin state or make both states thermally accessible. Trofimenko and his coworkers initiated the study of these systems by using a variety of techniques.[18] Thermochromic changes in solid $Fe[HB(pz)_3]_2$ led to the initial proposal that this complex undergoes a change in spin state upon heating.[19] Confirmation of this change was demonstrated by the large increase in its magnetic moment upon heating to ca. 400 K.[20] The room-temperature far-infrared

* Address correspondence to these authors at the University of Missouri—Rolla for G.J.L. and Abilene Christian University for B.B.H.

(1) Cambi, L.; Cagnasso, A. *Atti, Accad. Naz. Lincei, Cl. Sci. Fis. Mat. Natl., Rend.* **1931**, *13*, 809. Cambi, L.; Szego, L. *Ber. Dtsch. Chem. Ges. B* **1931**, *64*, 2591.
(2) Maki, G. *J. Chem. Phys.* **1958**, *28*, 651-662.
(3) Ballhausen, C. J.; Liehr, A. D. *J. Am. Chem. Soc.* **1959**, *81*, 538-542.
(4) Martin, R. L.; White, A. H. In *Transition Metal Chemistry*; Carlin, R. L., Ed.; Decker: New York, 1968; Vol. 4, pp 113-198.
(5) Gütlich, P. In *Mössbauer Spectroscopy Applied to Inorganic Chemistry*, Long, G. J., Ed.; Plenum: New York, 1984; Vol. 1, pp 287-337.
(6) Goodwin, H. A. *Coord. Chem. Rev.* **1976**, *18*, 293-325.
(7) Gütlich, P. *Struct. Bonding* **1981**, *44*, 83-202.
(8) König, E.; Ritter, G.; Kulshreshtha, S. K. *Chem. Rev.* **1985**, *85*, 219-234.
(9) König, E. *Prog. Inorg. Chem.* **1987**, *35*, 527-622.
(10) Pebler, J. *Inorg. Chem.* **1983**, *22*, 4125-4128.
(11) König, E.; Ritter, G.; Waigel, J.; Goodwin, H. A. *J. Chem. Phys.* **1985**, *83*, 3055-3061.
(12) Long, G. J.; Hutchinson, B. B. *Inorg. Chem.* **1987**, *26*, 608-613.
(13) Decurtins, S.; Gütlich, P.; Hasselbach, K. M.; Hauser, A.; Spiering, H. *Inorg. Chem.* **1985**, *24*, 2174-2178.
(14) Poganiuch, P.; Gütlich, P. *Inorg. Chem.* **1987**, *26*, 455-458.
(15) Gütlich, P. In *Chemical Mössbauer Spectroscopy*; Herber, R. H., Ed., Plenum: New York, 1984; pp 27-64.
(16) Wilson, D. F.; Dutton, P. L.; Erecinska, M.; Lindsay, J. G.; Sato, N. *Acc. Chem. Res.* **1972**, *5*, 234-241.
(17) Scheidt, W. R.; Reed, C. A. *Chem. Rev.* **1981**, *81*, 543-555.
(18) Jesson, J. P.; Trofimenko, S.; Eaton, D. R. *J. Am. Chem. Soc.* **1967**, *89*, 3158-3164.
(19) Jesson, J. P.; Weiher, J. F. *J. Chem. Phys.* **1967**, *46*, 1995-1996.
(20) Hutchinson, B.; Daniels, L.; Henderson, E.; Neill, P.; Long, G. J.; Becker, L. W. *J. Chem. Soc., Chem. Commun.* **1979**, 1003-1004.

0020-1669/89/1328-4406$01.50/0

spectrum of $Fe[HB(pz)_3]_2$ has been assigned through the use of iron-54 and iron-57 pure metal isotope substitution.[21] The room-temperature single-crystal X-ray structure[22] showed that the average low-spin Fe–N bond distance was 1.937 (7) Å and that the molecule has a distorted D_{3d} symmetry. The Mössbauer spectra of $Fe[HB(pz)_3]_2$, obtained[23] between 4.2 and 295 K, show a typical low-spin iron(II) doublet with a quadrupole splitting of 0.20 mm/s and an isomer shift decreasing from 0.48 to 0.41 mm/s.[12] However, at room temperature and applied pressures of 45 kbar and above, the Mössbauer spectrum reveals[12] up to 20% of a high-spin component with a quadrupole splitting of ca. 3.3 mm/s and an isomer shift of 0.87 mm/s.

Because of the thermochromic changes[19] and spin-state changes at high pressure,[12] and temperature,[20] we decided to study in detail the spin-state properties of $Fe[HB(pz)_3]_2$ above room temperature. In this paper we report a detailed study of an iron(II) compound that shows spin-state crossover above room temperature.

Experimental Section

The $Fe[HB(pz)_3]_2$ is the same sample used in our earlier studies,[12,21] which was prepared by the standard literature methods[24] by using ca. 90% enriched iron-57 obtained from Oak Ridge National Laboratory. It was sublimed at 463 K and 0.1 Torr immediately prior to use.

The infrared spectra were obtained by using a Digilab FTS-20C vacuum Fourier transform infrared spectrometer with a 6.25-μm mylar beam splitter. A triangular apodization function was used to eliminate spectral feet, and 500 scans were averaged for each spectrum. The high-temperature infrared spectra were obtained by using a resistively heated metal sample holder equipped with a constantan–copper thermocouple and polyethylene plates. The reference plates, which were ratioed against the sample spectra, matched the temperature of the sample. The temperature was allowed to stabilize for ca. 40 min after each heating and cooling stage. The optical spectra were measured in the same furnace with a Cary 14 spectrophotometer. For these measurements, the sample was dispersed unground between two thin layers of microcrystalline KBr and the resulting sandwich was pressed into a disk as described elsewhere.[25]

The diffuse-reflectance infrared spectra were obtained with a Harrick diffuse-reflectance accessory with a Harrick Model KKK vacuum chamber and variable-temperature control. The vacuum chamber has CsI windows. The reflectance sample was made up by mixing unground $Fe[HB(pz)_3]_2$ with freshly ground CsI in a 9:1 ratio. The surface of the sample was smoothed with a razor blade and the percent reflectance optimized by raising or lowering the sample pedestal in the vacuum chamber. The temperature was controlled by using a variable transformer and measured with a chromel–alumel thermocouple. The temperature was stabilized for 30 min at each temperature stage.

The differential scanning calorimetry measurements were obtained with a Perkin-Elmer DSC-4 and referenced to the melting point of indium. The temperature range from 323 to 473 K was scanned at 10 K/min in all measurements.

The magnetic susceptibilities were measured on a sample taken directly from the sublimation apparatus. For measurements above room temperature, the conventional Faraday method was used with a Cahn Model RM-2 electrobalance, a HdH/dx of 14 kg/cm, and $HgCo(NCS)_4$ as a calibrant. Heating of the sample was performed by using a tube wrapped with Cahn 7549 heating tape and controlled with a Valley Forge PC6011 temperature controller. The temperature was measured with a copper–constantan thermocouple. For measurements below room temperature, a Faraday balance[26] equipped with a Janis Supervaritemp cryostat, a Lake Shore Cryotronics temperature controller, and a silicon diode temperature sensor was used.

The Mössbauer spectra were obtained on a Harwell constant-acceleration spectrometer that utilized a room-temperature rhodium-matrix cobalt-57 source and was calibrated at room temperature with natural α-iron foil. Spectra above room temperature were obtained with a Ricor high-vacuum furnace and a Eurotherm temperature controller. The sample temperature was measured with a gold–cobalt thermocouple. The high-vacuum furnace was operated at ca. 10^{-5} Torr, and great care was exercised to ensure that the sample did not sublime onto the windows and radiation shields in the oven. After the high-temperature run, the sample container, a boron–nitride capsule, was removed from the furnace and the Mössbauer spectrum of the "blank" or empty furnace was measured. For all of the results reported herein, the resulting measurement showed no Mössbauer spectral absorption. Hence, it was certain that no sample had sublimed onto the shields or windows during the high-temperature measurements. Further, no sublimed material was observed visually inside the oven, indicating that little if any sublimation had occurred. It was found that it was essential to use a highly enriched iron-57 sample in order to obtain useful spectra above 400 K in a time period that minimized sample sublimation. Preliminary studies indicated that a highly ground sample sublimed quickly, even if mixed with boron nitride. Hence all measurements were obtained by using unground freshly sublimed samples. This has the disadvantage of yielding potential texture in the Mössbauer absorber, but the advantage of yielding useful spectra at higher temperatures. The absorber thickness was adjusted to give a percent effect of ca. 3% at the highest temperatures. The relatively large sample thickness was used in order to minimize spectral counting times at high temperature, but did lead to high percent effects at lower temperatures. Analogous experiments with thinner absorbers led to hyperfine parameters essentially identical with those reported herein at temperatures below ca. 400 K. Spectral counting times ranged from 30 min near room temperature to ca. 4 h above 400 K. Below 400 K, the temperature was allowed to stabilize for at least 60 min between each spectral measurement. Above 400 K, the time interval was reduced to 30 min to minimize any sublimation. The resulting spectra were fit either with quadrupole doublets with a Lorentzian line shape or with a relaxation line-shape profile by using standard least-squares computer minimization techniques. The relaxation fits were based on the method reported by Litterst and Amthauer[27] for relaxation between two quadrupole split doublets representing the low-spin and high-spin electronic states. The sum of the high-spin population and the low-spin population was 1, and the conditions that the relaxation rate, λ_+, from the low-spin state to the high-spin state times the low-spin state population, p_{LS}, was equal to the relaxation rate, λ_-, from the high-spin state to the low-spin state times the high-spin state population, p_{HS}, i.e.

$$p_{LS} + p_{HS} = 1 \qquad \lambda_+ p_{LS} = \lambda_- p_{HS}$$

were fulfilled in these fits. Hence, there are only two independent parameters, p_{LS} and λ_-, henceforth referred to as λ. The quadrupole splitting of the low-spin doublet in these relaxation fits was kept constant at 0.17 mm/s, a value close to that observed[12] at low temperature. The line width for each doublet was fixed at 0.39 mm/s in all the relaxation fits. This value is rather large, but not unreasonable for thick absorbers. There is a high correlation coefficient between the experimental line width and the relaxation rates. We believe that the resulting hyperfine spectral parameters are accurate to ca. ±0.02 mm/s.

The volume expansion was measured on a Perkin-Elmer Thermal Mechanical PMS-2 analyzer.

Results and Discussion

Variable-Temperature Infrared Spectroscopy. Earlier work[21] on the solid-state infrared spectrum of $Fe[HB(pz)_3]_2$ at 295 and 77 K showed no significant changes with temperature for the bands above 625 cm^{-1}, and consequently these bands were assigned primarily to ligand vibrations. Two bands at 434.5 and 399.5 cm^{-1} were identified as Fe–N stretching bands because of their metal isotopic shifts of 5.0 and 4.9 cm^{-1}, respectively.[21] In addition, an absorption of weak intensity, occurring at 459 cm^{-1}, shows a metal isotopic shift of about 5 cm^{-1} and is also assigned as an Fe–N stretching band. The 459-cm^{-1} band was not studied at higher temperatures in this work because of its weak intensity. The remainder of the far-infrared spectrum showed no bands with a significant metal isotope dependence, and as expected, few changes were observed as the temperature was lowered from 295 to 77 K.

In contrast, significant changes in the infrared spectrum of $Fe[HB(pz)_3]_2$ appeared as the temperature was increased from 295 to 466 K. A comparison of the spectra obtained at 295 and 466 K is shown in Figure 1. These changes may be accounted for by a spin-state crossover with increasing temperature and its

(21) Hutchinson, B.; Hoffbauer, M.; Takemoto, J. *Spectrochim. Acta* **1976**, *32A*, 1785–1792.
(22) Oliver, J. D.; Mullica, D. F.; Hutchinson, B. B.; Milligan, W. O. *Inorg. Chem.* **1980**, *19*, 165–169.
(23) Jesson, J. P.; Weiher, J. F.; Trofimenko, S. *J. Chem. Phys.* **1968**, *48*, 2058–2066.
(24) Trofimenko, S. *J. Am. Chem. Soc.* **1967**, *89*, 3170–3177. Jesson, J. P.; Trofimenko, S.; Eaton, D. R. *J. Am. Chem. Soc.* **1967**, *89*, 3148–3158.
(25) Wrobleski, J. T.; Long, G. J. *Appl. Spectrosc.* **1977**, *31*, 177–179.
(26) Long, G. J.; Longworth, G.; Battle, P.; Cheetham, A. K.; Thundathil, R. V.; Beveridge, D. *Inorg. Chem.* **1979**, *18*, 624–632.
(27) Litterst, F. J.; Amthauer, G. *Phys. Chem. Miner.* **1984**, *10*, 250–255.

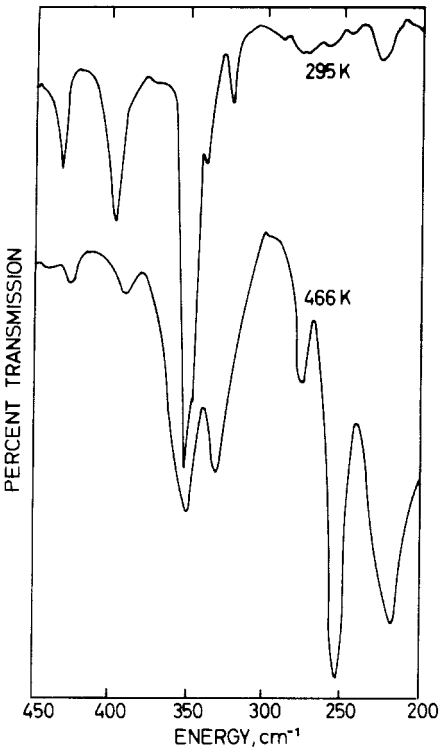

Figure 1. Infrared spectra of $Fe[HB(pz)_3]_2$ obtained at 295 and 466 K.

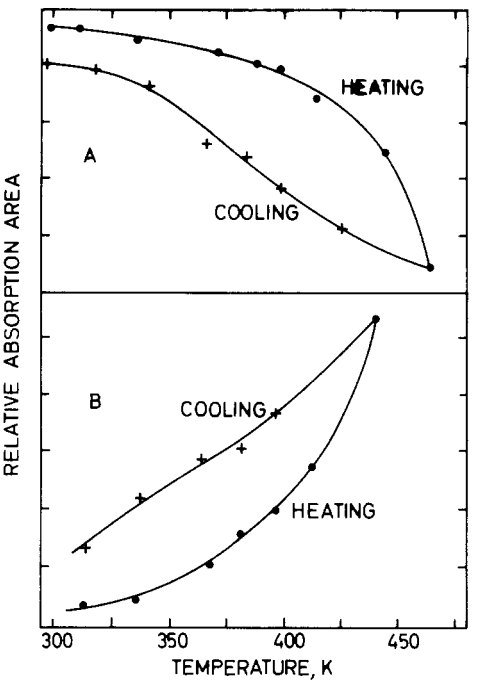

Figure 2. Relative change in the intensity of the 399.5- (A) and 257.5-cm^{-1} (B) Fe–N vibrational bands in $Fe[HB(pz)_3]_2$ with temperature.

effect on the Fe–N bond length and distance as reflected in the Fe–N vibrational stretching frequencies.

The low-spin Fe–N stretching bands observed at 434.5 and 399.5 cm^{-1} at 295 K have decreased markedly in area and have shifted to slightly lower energy at 466 K. A plot of the change in the relative area of the 399.5 cm^{-1} absorption band with temperature is shown in Figure 2A. The decrease in absorption area is not linear but shows a temperature dependence similar to that observed[20] for the magnetic susceptibility (see below). When $Fe[HB(pz)_3]_2$ is cooled to room temperature, the area of this band shows a hysteresis and returns to only ca. 80% of its original area at 295 K. During the initial heating this band broadens from 8 to 12 cm^{-1} at half-height at 466 K and does not narrow upon cooling to 295 K. The 5-cm^{-1} decrease in the band position upon heating is reversible upon cooling. The second major low-spin Fe–N stretching band appears at 434.5 cm^{-1} in an absorption envelope that contains a weak shoulder at 444 cm^{-1}. The same decrease in intensity with increasing temperature, as observed in Figure 2A, occurs for this band. When the sample is cooled from 466 to 295 K, this absorption band also regains most of its original intensity, showing an analogous broadening and small frequency decrease upon heating.

The infrared absorptions due to the high-spin Fe–N stretch are expected to occur at a lower energy than the low-spin Fe–N stretching bands. The two electrons in the antibonding e_g orbitals of the high-spin $t_{2g}^4e_g^2$ configuration weaken the iron–nitrogen bond, thus lowering its stretching frequencies. This is confirmed by the infrared spectrum[24] of $Fe[HB(3,5\text{-}(CH_3)_2pz)_3]_2$ which is high spin[12] at all temperatures and exhibits Fe–N stretching bands only in the 200–260-cm^{-1} region.

The high-spin Fe–N stretching bands in $Fe[HB(pz)_3]_2$ should appear in the 200–260-cm^{-1} region, but they will be weak in intensity at room temperature because the complex is primarily in the low-spin configuration. As noted below, absorption bands other than Fe–N stretching bands show an increase in intensity upon heating, and consequently, band assignments cannot be based solely on their temperature dependence. At 466 K the two absorption bands that appear in the spectrum of $^{54}Fe[HB(pz)_3]_2$ at 256.0 and 222.9 cm^{-1} shift by 4.2 and 2.9 cm^{-1} upon iron-57 substitution. On this basis, we assign these bands to the high-spin Fe–N stretch. The first absorption at 295 K in the 200–260-cm^{-1} region occurs at 257.5 cm^{-1}. The area of this band, as shown in Figure 2B, increases to a maximum at 466 K. The energy of this band shows a reversible decrease in frequency of 2.5 cm^{-1} when the sample is heated. After one heating and cooling cycle, the intensity of this band has increased from 5% to 22% (see Figure 2B). Therefore, we have been able to distinguish and directly assign, by using isotopic measurements, both the low-spin Fe–N stretching bands at room temperature and the high-spin Fe–N stretching bands at high temperature. The 200-cm^{-1} difference in the Fe–N stretching band position clearly illustrates the decrease in bond strength from the low-spin to the high-spin form.

The other major room-temperature absorption band appearing in this region is at 223 cm^{-1}. This band exhibits a temperature behavior very similar to that of the 257.5-cm^{-1} band, and its area is twice as large at 295 K after one heating and cooling cycle. The plot of intensity of the low-spin Fe–N stretching bands is similar to the heating and cooling cycle found by Mössbauer and magnetic moment analyses.

Several infrared absorption bands have less than 1-cm^{-1} metal isotopic dependence, but their intensities are temperature dependent and appear in the region of the Fe–N stretching bands. Two of these bands at 275 and 337 cm^{-1} show a significant increase in area with increasing temperature and can be associated with the high-spin state of $Fe[HB(pz)_3]_2$. A band at 325 cm^{-1} decreases in intensity with increasing temperature and thus is associated with the low-spin state. The temperature dependence of these three bands is smoother than that observed for the Fe–N stretching bands, possibly because they are less directly affected by the spin-state crossover. A fourth band at 350 cm^{-1} broadens significantly from 10 cm^{-1} at half-height at 295 K to 22 cm^{-1} at 466 K. The assignment of this absorption is not clear.

The effect of mechanical grinding can influence the characteristics of the spin-state crossover.[15] The preparation of a mull for infrared spectroscopy includes the grinding of the sample. To evaluate the effect of grinding on the shape of the band intensity vs temperature, diffuse-reflectance spectroscopy was employed. Diffuse-reflectance spectroscopy provides an infrared spectrum without sample grinding.[28] Although the absorption bands were not as intense as in the mull sampling method, the decrease in the area of the Fe–N stretching band at 399.5 cm^{-1} could be readily observed as the temperature was increased. The results indicate a sharper decrease in the area of the 399.5-cm^{-1} band upon heating, presumably due to the larger crystal size present

(28) Fuller, M. P.; Griffiths, P. R. *Anal. Chem.* **1978**, *50*, 1906–1910.

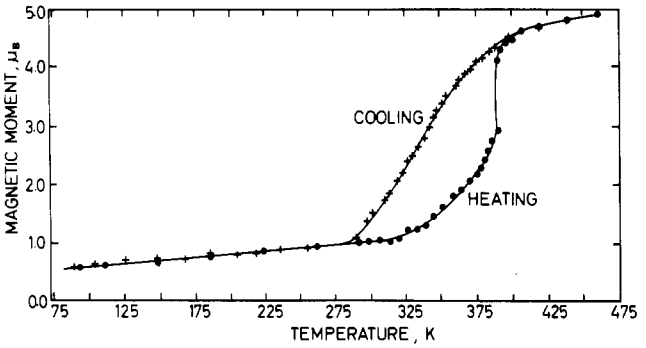

Figure 3. Temperature dependence of the magnetic moment for $Fe[HB(pz)_3]_2$ during heating and cooling.

in the absence of grinding, but no other significant differences.

The changes observed in the intensity of the high-spin and low-spin vibrational bands with temperature are of course qualitatively related to the spin-state crossover. It is tempting to propose a quantitative relationship between the populations of the various states as measured via the infrared vibrational spectra, the Mössbauer spectra, and the magnetic susceptibility results (see below). However, we chose not to do this because the infrared results are not obtained on the pure material, but rather in a mull that requires grinding or a sample KBr disk made at high-pressure. In the case of the diffuse-reflectance spectra, the relative intensities are highly influenced by the anisotropic nature of the sample used and the changes in crystallite size associated with the phase transition. However, we can learn something about the spin-state crossover because the nearly constant energy of both the low-spin and high-spin Fe–N vibrational stretching bands during heating supports the cooperative domain model of spin-crossover described by Sorai and Seki.[29] In their model the major driving force for the spin-state transition in $Fe[HB(pz)_3]_2$ is the entropy difference between the two spin states. The typical total entropy change for these transitions has been measured by two methods[18,30] and found to be in the range of 48–55 J/(K mol). The entropy change due to the difference in the high-spin and low-spin Fe–N vibrational bands observed in this work provides 20 J/(K mol) of the total entropy change. This value is obtained by assuming all four vibrational bands are E modes and by calculating the vibrational contribution to the entropy with the vibrational partition function.[31,32] In addition, there is a 13.4 J/(K mol) contribution to the total entropy from the magnetic contribution to the spin-state crossover.[18,30]

Magnetic Susceptibility Studies. The magnetic properties of $Fe[HB(pz)_3]_2$ have been reported[20] earlier for temperatures above 300 K. We have now extended these studies to lower temperature, and the results are shown in Figure 3 and the magnetic moments are given in Table I.[33] The magnetic moment of a freshly sublimed sample of $Fe[HB(pz)_3]_2$ exhibits a slow but steady increase from 0.60 μ_B at 91.3 K to 2.90 μ_B at 389 K at which point the moment increases sharply to 4.14 μ_B at 390 K and then gradually increases to 4.91 μ_B at 461 K. Upon cooling, the moment decreases gradually to 1.38 μ_B at 298 K and to 0.61 μ_B at 90.2 K. Figure 3 indicates that the magnetic moment shows no sharp decrease upon cooling but decreases uniformly, reaching a value close to the initial moment only at ca. 250 K. The moment exhibits a distinct hysteresis upon the initial heating and cooling. However, subsequent heating of the sample yields moments that follow the initial *cooling* curve. These results are most consistent with a ground state admixture of the $^1A_{1g}$ and $^5T_{2g}$ electronic spin-states with the population of the $^5T_{2g}$ state gradually increasing up to 389 K. At this point $Fe[HB(pz)_3]_2$ undergoes a crystallographic phase transition (see below), and the initial well-formed crystals shatter into extremely small fragments. The phase transition is accompanied by a change in the electronic ground state to an essentially high-spin configuration as indicated by the moment, which approaches the spin-only value for iron(II) at 461 K. Upon cooling, there is a continuous change in the relative population of the high-spin and low-spin states in the admixture making up the electronic ground state. The difference in the populations of the two states upon heating and cooling must result from the large change in crystallite volume occurring at the phase transformation. Similar effects are observed in the Mössbauer spectral properties as discussed below.

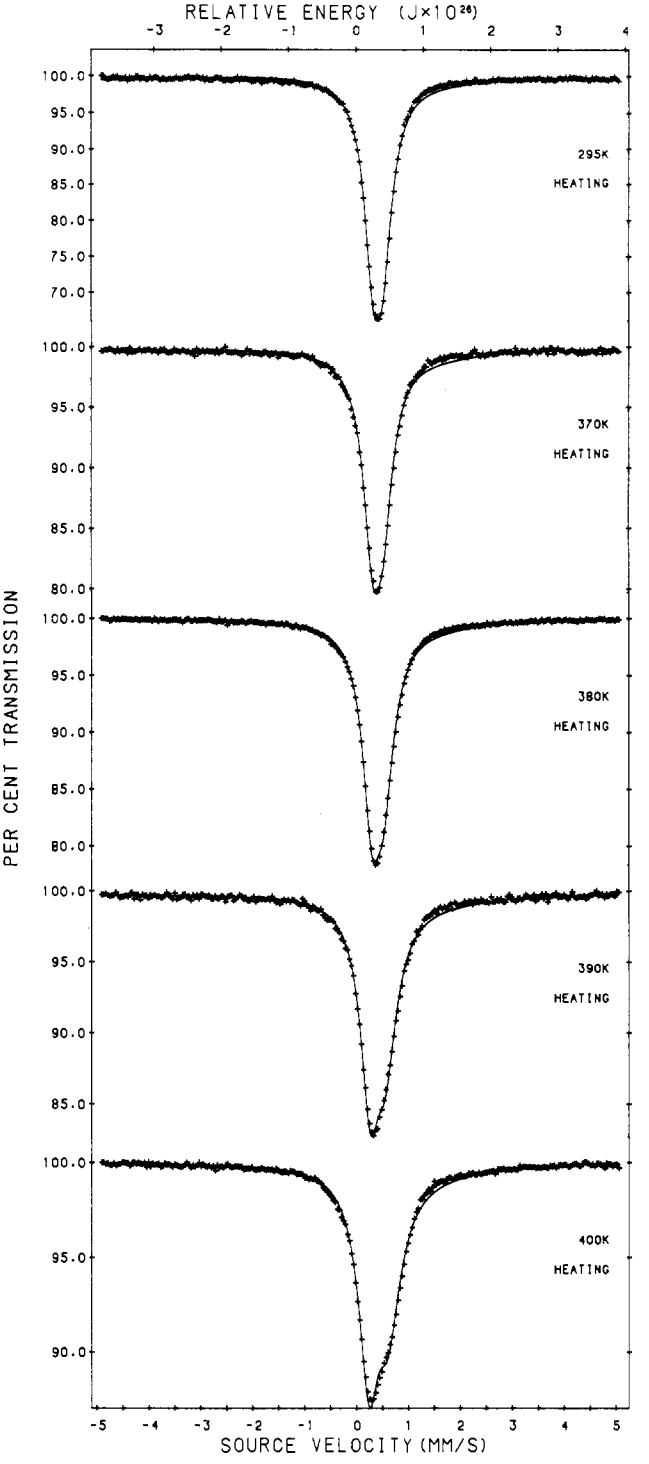

Figure 4. Mössbauer spectra of $Fe[HB(pz)_3]_2$ obtained between 300 and 400 K during the first heating and fit with a relaxation model.

It is possible to estimate the relative contributions of the two spin-states to the ground state, if the moments of the high-spin and low-spin states are known. From the temperature dependence

(29) Sorai, M.; Seki, S. *J. Phys. Chem. Solids* **1976**, *35*, 555–570.
(30) Beattie, J. K.; Binstead, R. A.; West, R. J. *J. Am. Chem. Soc.* **1978**, *100*, 3044–3050.
(31) Herzberg, G. *Infrared and Raman Spectra of Polyatomic Molecules*; D. Van Nostrand Co, Inc.: New York, 1945; pp 522–523.
(32) Wilson, E. B. *Chem. Rev.* **1940**, *27*, 17–38.
(33) See paragraph at end of paper regarding supplementary material.

Table II. Mössbauer Effect Hyperfine Parameters Obtained with the Relaxation Model[a]

	low-spin component		high-spin component			eff relaxn	eff relaxn	abs area,
T, K	δ[b]	% A	δ[b]	ΔE_Q	% A	rate, mm/s	rate, MHz	%ϵ(mm/s)
295[c]	0.43	98	0.94	3.55	2	0.039	2.0	25.3
350[c]	0.41	96	0.87	3.25	4	0.075	3.9	19.7
360[c]	0.40	95	0.87	3.24	5	0.156	8.0	19.1
370[c]	0.42	92	0.86	3.18	8	0.128	6.6	17.1
380[c]	0.41	87	0.86	3.12	13	0.278	14.3	16.8
390[c]	0.40	81	0.86	3.11	19	0.523	26.8	16.1
400[c]	0.41	76	0.82	2.97	24	0.715	36.7	14.2
405[c]	0.40	72	0.74	2.97	28	0.926	47.5	12.9
407.5[c]	0.35	38	0.79	2.85	62	0.605	31.0	7.7
410[c]	0.32	31	0.80	2.91	69	0.973	49.9	6.7
413[c]	0.34	32	0.82	3.01	68	1.098	56.3	6.7
415[c]	0.47	31	0.83	3.05	69	1.355	69.5	6.4
420[c]	0.45	30	0.82	3.04	70	0.992	50.9	6.1
430[c]	0.43	29	0.85	3.15	71	1.008	51.7	5.6
420[d]	0.44	31	0.84	3.09	69	0.976	50.1	5.9
400[d]	0.50	38	0.86	3.09	62	1.044	53.5	7.0
390[d]	0.44	42	0.86	3.10	58	1.668	85.5	7.6
380[d]	0.45	46	0.88	3.12	54	1.527	78.3	8.5
370[d]	0.44	51	0.87	3.12	49	1.219	62.5	9.6
360[d]	0.45	56	0.87	3.24	44	1.008	51.7	10.5
355[d]	0.44	59	0.85	3.23	41	0.824	42.3	11.4
350[d]	0.45	61	0.87	3.25	39	0.723	37.1	11.1
340[d]	0.45	64	0.86	3.32	36	0.527	27.0	11.5
330[d]	0.46	67	0.87	3.30	33	0.422	21.6	11.7
320[d]	0.45	68	0.86	3.44	32	0.384	19.7	11.9
310[d]	0.45	71	0.87	3.56	29	0.361	18.5	11.5
296[d]	0.46	74	0.94	3.55	26	0.277	14.2	11.6

[a] All parameters are given in mm/s unless otherwise indicated. In the model the line width of all lines was constrained to be 0.39 mm/s at all temperatures and the quadrupole splitting of the low-spin component was fixed at 0.17 mm/s (see text). [b] The isomer shift is relative to that of room-temperature natural α-iron foil. [c] Initial heating. [d] Cooling.

of the moments, we have estimated values of 0.60 μ_B for the low-spin electronic configuration and 5.1 μ_B for the high-spin electronic configuration. The resulting populations of each spin-state in the ground state are given in Table I[33] and are similar to the populations obtained from the Mössbauer spectral fits (see below).

Mössbauer Spectral Studies. The Mössbauer spectra of Fe[HB(pz)$_3$]$_2$ obtained on a freshly sublimed, crushed, but unground sample (see Experimental Section), which had not been previously heated, are shown in Figures 4 and 5.[34] The Mössbauer effect spectral parameters are presented in Tables II and III.[34] The resulting symmetric spectra obtained from 295 to 370 K are typical of a low-spin iron(II) complex and the hyperfine parameters are similar to those reported earlier[12,18,19] for Fe[HB(pz)$_3$]$_2$. However, the spectra obtained at 380, 390, and 400 K and the central component observed at 405 K show a distinctly asymmetric line shape and may not be fit with a symmetric quadrupole doublet. Our best fits with an asymmetric quadrupole doublet, illustrated in Figure 4A[34] indicate that the component lines have identical areas and very different, rather large, line widths. This indicates that the observed spectra are the result of rapid relaxation on the Mössbauer time scale of 10^{-8} s between the low-spin and high-spin states.[35] The results for such a relaxation fit are shown in Figure 4, and the hyperfine parameters corresponding to these fits are given in Table II. Although these fits are not as good as the doublet fits, they are consistent with the magnetic data, which indicate that the ground state consists of a temperature-dependent population of both the low-spin and high-spin electronic configurations. The structure observed in the spectra at 405 and 407.5 K, as shown in Figure 5, seems to argue against this rapid relaxation. However, it appears, especially at 405 K, that the spectra reveal the presence of both the low-temperature and high-temperature phases of Fe[HB(pz)$_3$]$_2$.

The influence of the phase transition is obvious in the Mössbauer spectra obtained at 405, 407.5, and 410 K. Between 405 and 410 K the broad line at ca. 0.5 mm/s virtually disappears and is replaced by a quadrupole doublet with a large splitting typical of high-spin iron(II), as is illustrated in Figure 5. Further increases in the temperature up to 430 K yield only minor changes in the observed spectra. The spectra in this temperature range can be fit either with two quadrupole doublets, with very large line widths, as illustrated in Figure 5A[34] or with a rapid relaxation model, Figure 5.[36] In all the relaxation fits, the low-spin state quadrupole interaction has been constrained to 0.17 mm/s and the line width of all lines has been fixed at 0.39 mm/s. It is difficult to chose between the two models, but the magnetic data, the Mössbauer data obtained on cooling (see below), and the more reasonable line width used in the relaxation fits support the presence of rapid relaxation between the two spin states on the Mössbauer time scale.

When the sample is cooled from 430 K the Mössbauer spectra observed for Fe[HB(pz)$_3$]$_2$ are totally different from those observed upon heating. This is best seen in a comparison of the spectra obtained upon heating to 370 and 380 K, Figure 4, with those obtained upon cooling to 370 and 380 K, Figure 6. At all temperatures between 400 and ca. 340 K, a very broad absorption envelope is observed upon cooling. It has proven impossible to fit this broad absorption with two quadrupole doublets with any reasonable hyperfine parameters and line widths, and we have been forced to use the electronic spin-state relaxation model to

(34) The fits with quadrupole doublets are shown only in the supplementary material as Figures 4A and 5A. The resulting hyperfine parameters are given in the supplementary material as Table III.

(35) There are several possible alternative explanations for this asymmetry. First, it could arise from a difference in the temperature dependence of the two crystallographically distinct iron sites in Fe[HB(pz)$_3$]$_2$. Second, it could be the result of texture in the unground samples. Third, it could be due to the Goldanskii–Karyagin effect arising from an anisotropy in the recoil-free fraction, an anisotropy expected to increase with increasing temperature. The data are probably consistent with all three possibilities; however, each of these explanations seems unlikely in view of the structure of the compound and the success obtained with the relaxation model.

(36) The fits with two doublets are better, at least in part, because in these fits, 10 parameters, the four peak positions and line widths, their relative area, and the total area, are adjusted. In contrast, in the relaxation model, only six parameters, the isomer shifts of the high-spin and low-spin states, the quadrupole splitting of the high-spin state, the population of the high-spin state, the relaxation rate, and the total area, are adjusted.

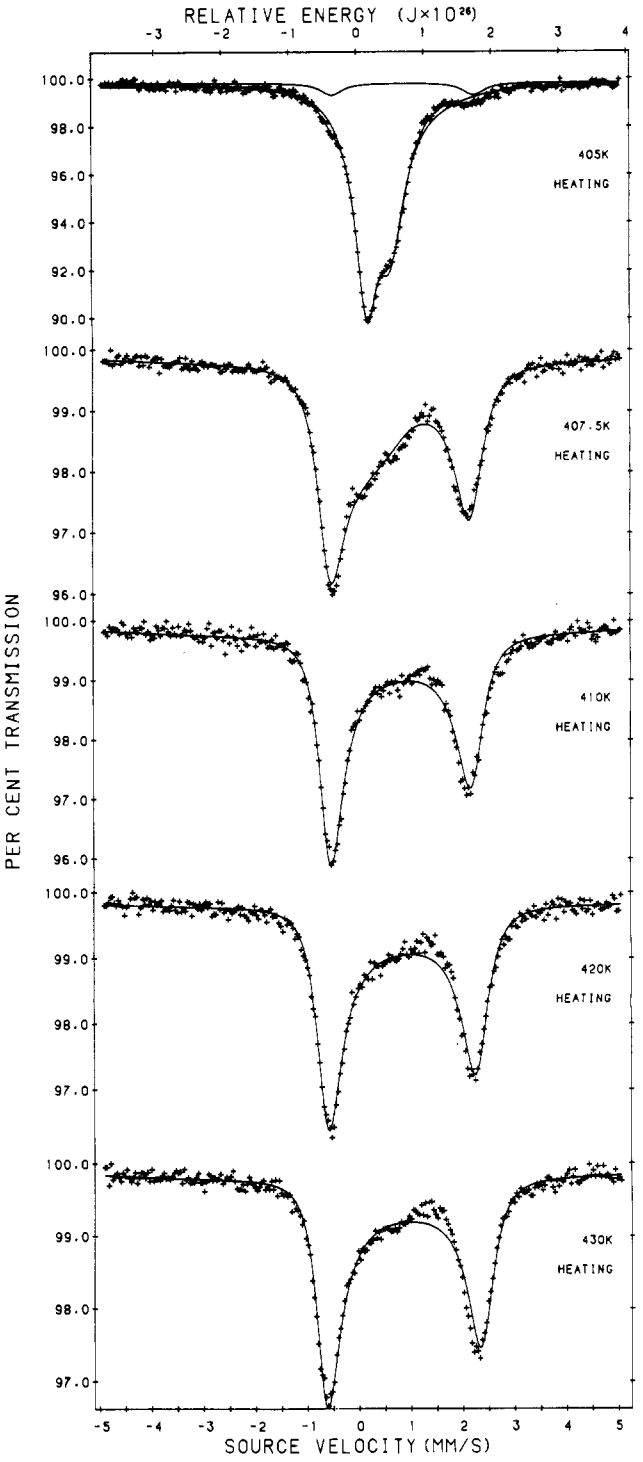

Figure 5. Mössbauer spectra of $Fe[HB(pz)_3]_2$ obtained between 405 and 430 K during the first heating and fit with a relaxation model.

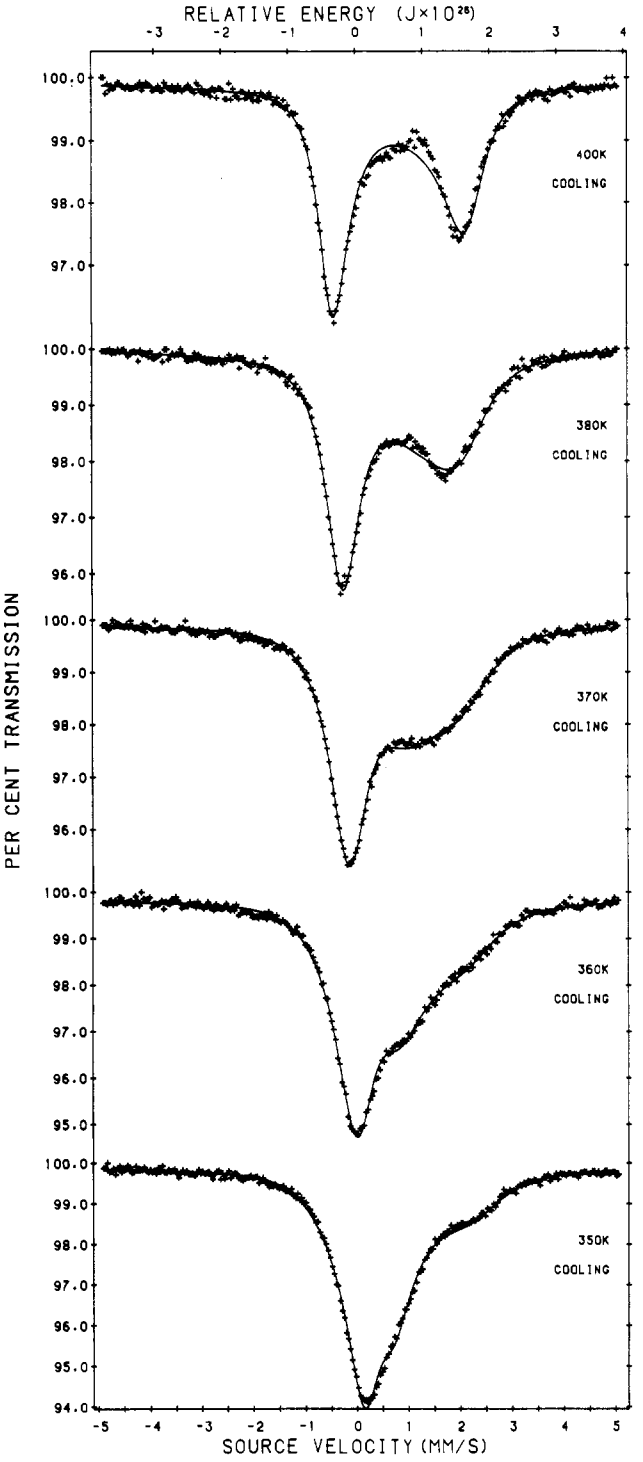

Figure 6. Mössbauer spectra of $Fe[HB(pz)_3]_2$ obtained between 400 and 350 K during cooling and fit with a relaxation model.

understand these spectra. The results of this relaxation fit are shown by the solid lines in Figures 6 and 7, and the hyperfine parameters, relaxation rates, and spin-state populations are given in Table II. The quality of these fits, although not perfect at 380 K, is excellent at all other temperatures. In Table II, we give the effective relaxation rate in millimeters per second obtained for our fits, which used an effective line width of 0.39 mm/s. In order to compute the effective relaxation rate in megahertz, we have used the well-known correspondence of the natural line width of iron-57 of 0.195 mm/s to 10 MHz. Because the line width used in our fits is twice the natural line width, the resolution in time of our measurements is changed by a factor of 2 and the effective relaxation rate in megahertz, given in Table II, should thus be divided by a factor of 2. In principle, a more advanced treatment of the spectra should be carried out in order to eliminate the use of the large line width in the fits. Such a treatment would involve computing a distribution of relaxation spectra and using the convolution integral to correct for the line broadening resulting from the thick absorber. Such a complex treatment was not attempted herein, and consequently, the absolute values of the relaxation rate should be taken with caution.

The hyperfine parameters obtained in the relaxation fits are all quite normal for iron(II) in a compound undergoing a spin-state crossover. The relaxation model yields the relative populations of the two states as well as the relaxation rate between the two states. A plot of the population of the high-spin state, derived from these relaxation fits upon heating and cooling, is shown in Figure 8. There is a striking resemblance between this plot and the experimental magnetic moments shown in Figure 3. Further, there is qualitative agreement in the populations as derived from

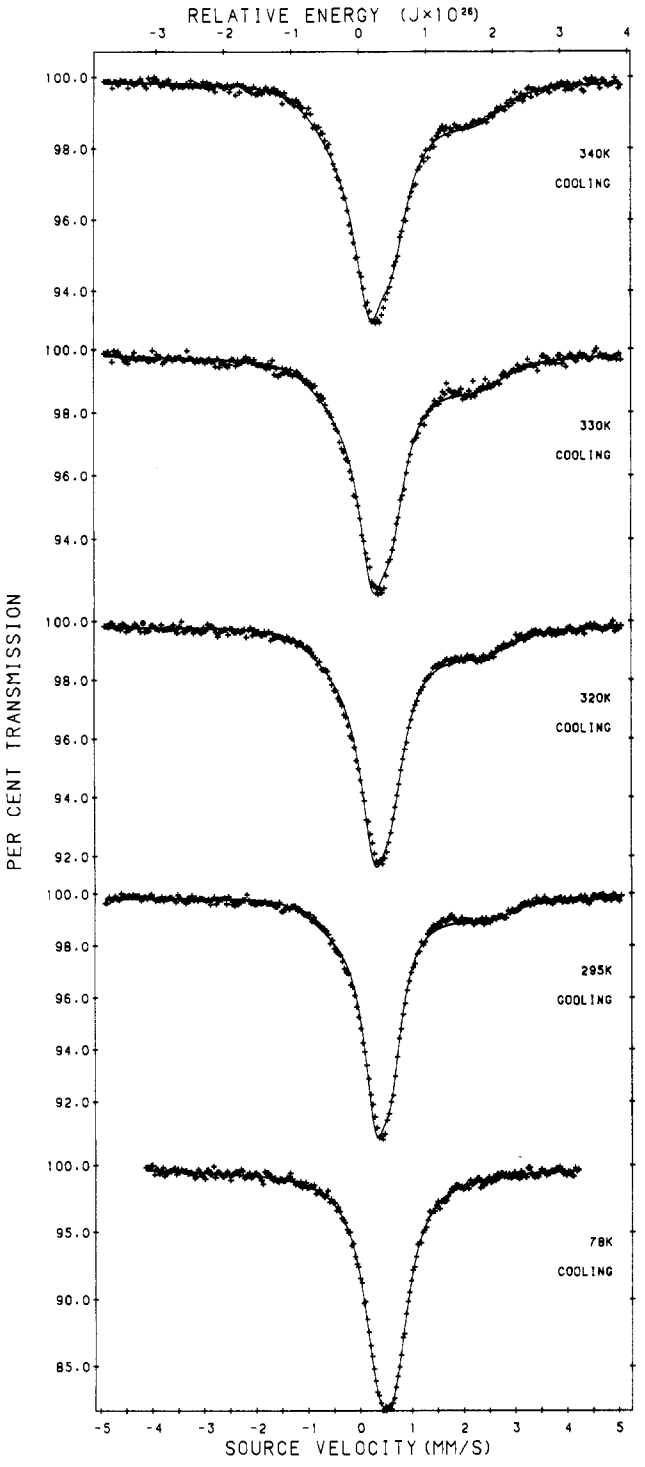

Figure 7. Mössbauer spectra of $Fe[HB(pz)_3]_2$ obtained between 340 and 78 K during cooling and fit with a relaxation model.

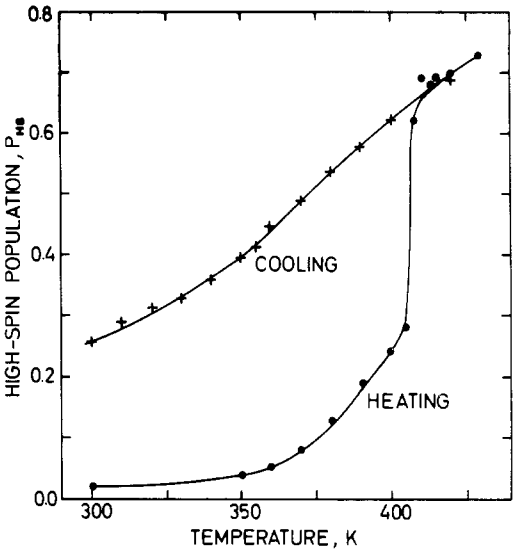

Figure 8. Relative population of the high-spin state in $Fe[HB(pz)_3]_2$ as determined from the Mössbauer spectra as fit with a spin-state relaxation model.

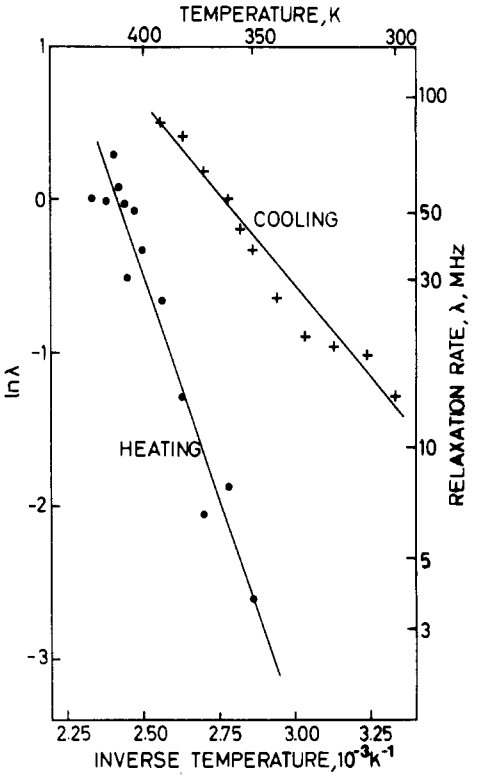

Figure 9. A Plot of the logarithm of the relaxation rate vs $1/T$ for $Fe[HB(pz)_3]_2$.

the magnetic moments and Mössbauer spectra, especially when one considers the approximations involved in obtaining the values from the moments.

A plot of the natural logarithm of the relaxation rate vs the inverse temperature is given in Figure 9. It is apparent from this plot that the activation energy for relaxation is different for the initial heating of the crystals, before the phase transition occurs, and for cooling after the phase transition has shattered the crystals. The slopes of the plots yield an activation energy of 10 500 K or 7300 cm^{-1} during the heating of the large single crystals and a value of 2530 K or 1760 cm^{-1} during the cooling of the much smaller crystals present after heating. The "cooperative" nature of the spin-state transition and the accompanying crystallographic phase transition is indicated by the sharp increase in the population of the high-spin state shown in both Figures 3 and 8 and is further anticipated by the large activation energy observed below the transition. Although electronic spin-state relaxation on the Mössbauer time scale is unusual for iron(II) compounds in the solid state,[37] relaxation rates very similar to those found herein for $Fe[HB(pz)_3]_2$ have been observed for several iron(III) complexes.[38,39] It is interesting to note that in one of these cases,[39] $[Fe(acpa)_2]PF_6$, the rapid electronic relaxation is also associated with a crystallographic phase transformation. In a more recent study of an iron(II) compound, Adler et al.[40] found that [Fe-

(37) Grandjean, F. In *The Time Domain in Surface and Structural Dynamics*; Long, G. J., Grandjean, F., Eds., Kluwer Academic Publishers: Boston, MA, 1988; pp 287–308.
(38) Maeda, Y.; Tsutsumi, N.; Takashima, Y. *Inorg. Chem.* **1984**, *23*, 2440–2447.
(39) Maeda, Y.; Oshio, H.; Takashima, Y.; Mikuriya, M.; Hidaka, M. *Inorg. Chem.* **1986**, *25*, 2958–2962.
(40) Adler, P.; Spiering, H.; Gütlich, P. *Inorg. Chem.* **1987**, *26*, 3840–3845.

(2-(aminomethyl)pyridine)$_3$]$(PF_6)_2$ undergoes relaxation on the iron-57 Mössbauer effect time scale in the temperature range between approximately 200 and 290 K. Their analysis yielded an activation energy of 2480 K or 1720 cm^{-1} for the high-spin to low-spin transition. The value we obtain for $Fe[HB(pz)_3]_2$ upon cooling after the phase transition is virtually the same, but the activation energy for the freshly sublimed material upon its initial heating is substantially larger.

The difference in the relaxation rate and activation energies between the two electronic spin states and hence in the Mössbauer spectra obtained on heating and cooling may be understood in terms of the physical changes that occur in the crystals during the crystallographic phase change that occurs on heating. A visual microscopic examination of the crystal both before and after the heating indicates that, at the phase transition, the large well-formed single crystals of sublimed $Fe[HB(pz)_3]_2$ are shattered to yield an extremely fine polycrystalline powder. We estimate that the largest dimension of the microcrystals obtained after heating is at most 1% of that of the unheated sublimed sample. Our results from the magnetic measurements and the infrared and Mössbauer spectral studies indicate that the initial spin-state crossover is a cooperative phenomenon that depends upon crystallite size. After the crystals have shattered at the phase transition, the activation energy for the electronic relaxation between the two spin states is reduced by a factor of 3–4, perhaps as a result of a substantial decrease in the lattice elastic energy,[41] which may be stored in the crystals after their size has been greatly reduced. As a result, the electronic environment at a specific iron(II) site is free to fluctuate on the Mössbauer time scale between the high-spin and low-spin states. On continued cooling, the Boltzmann population of the higher energy, high-spin, $^5T_{2g}$ electronic state is reduced, the influence of the relaxation averaging is reduced, and the observed Mössbauer spectra gradually approach that expected for the low-spin iron(II) compound.

Finally it should be noted that, upon subsequent reheating, the Mössbauer spectra are essentially the same as those obtained upon the initial cooling (see Figures 6 and 7) and show no sharp change as is observed upon the initial heating of the sublimed material.

Optical Absorption Spectra. The optical absorption spectra of $Fe[HB(pz)_3]_2$, obtained upon heating and cooling, are shown in Figure 10. The 298 K spectrum is dominated by a very intense charge-transfer band in the ultraviolet region and also shows a less intense band centered at 19000 cm^{-1}. These intense absorptions account for the deep violet color of $Fe[HB(pz)_3]_2$ at room temperature. As the temperature increases, the absorbance at the peak of this band remains relatively constant (see Figure 11) up to ca. 390 K, above which its absorbance decreases sharply; a decrease which is without doubt associated with the crystallographic phase transition occurring at ca. 400 K. This change may be easily observed visually as the crystals change from deep violet to white between 390 and 410 K. Upon subsequent cooling, the absorbance at the peak maximum increases gradually until, at lowest temperatures, it actually exceeds that of the unheated sample (Figure 11), although the integrated intensity under the band is essentially the same as that in the unheated sample. These results indicate that $Fe[HB(pz)_3]_2$ maintains its predominantly low-spin $^1A_{1g}$ electronic ground state at temperatures up to 390 K at which point the phase transition and electronic spin-state crossover occur with a sharp decrease in the population of the $^1A_{1g}$ state and hence decrease in the 19000-cm^{-1} absorption band. Upon cooling, there is a gradual decrease in the population of the high-spin state and an increase in the population of the low-spin state in the admixture making up the electronic ground state in agreement with the gradual changes found in the magnetic moments and the infrared and Mössbauer spectra. Upon subsequent reheating, the absorbance follows the cooling path shown in Figure 11. The reason for the decrease in the line width of the 19000-cm^{-1} band upon heating is uncertain, but may be related to the large decrease in crystallite size at the phase transition as the crystallites shatter.

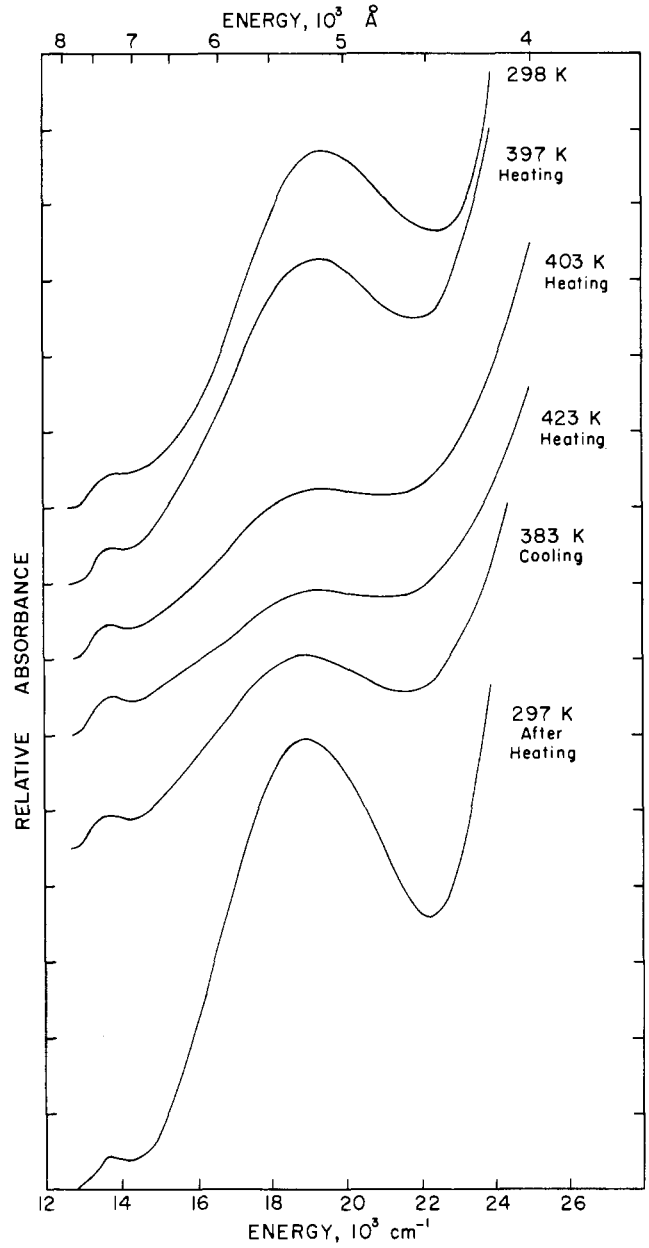

Figure 10. Optical absorption spectra of $Fe[HB(pz)_3]_2$ obtained at several temperatures upon heating and cooling.

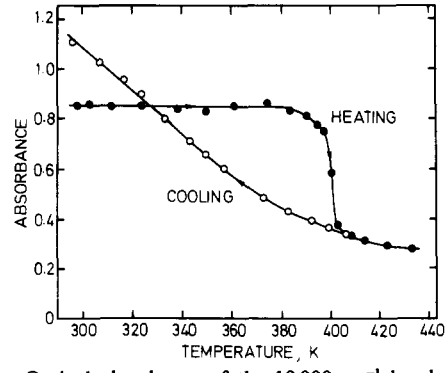

Figure 11. Optical absorbance of the 19000-cm^{-1} band observed in $Fe[HB(pz)_3]_2$ as a function of temperature.

Differential Scanning Calorimetry. The differential scanning calorimetry curve for a freshly sublimed sample of $Fe[HB(pz)_3]_2$ is shown in Figure 12 and clearly indicates the presence of a phase transition centered at 432 K with the onset of the transition

(41) Spiering, H.; Meissner, E.; Köppen, H.; Müller, E. W.; Gütlich, P. *Chem. Phys.* **1982**, *68*, 65–71. Adler, P.; Wiehl, L; Meissner, E.; Köhler, C. P.; Spiering, H.; Gütlich, P. *J. Phys. Chem. Solids* **1987**, *48*, 517–525.

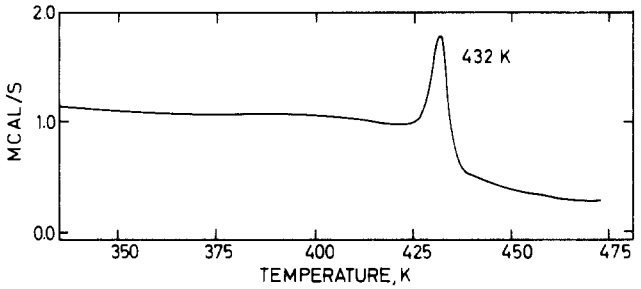

Figure 12. Differential scanning calorimetry curve obtained for freshly sublimed $Fe[HB(pz)_3]_2$.

occuring at 424 K. Measurement of several preparations of $Fe[HB(pz)_3]_2$ shows that no thermal changes occur below the endothermic peak at 432 K. However, depending on the preparation, this temperature may be as much as 7 K lower but has never been observed at higher temperatures. A simultaneous DTA-TGA analysis of freshly sublimed $Fe[HB(pz)_3]_2$ revealed no change in mass associated with this endotherm, which is thus assigned to the crystallographic phase transformation.

Jesson et al.[23] noted that the difference in volume for two different spin states can cause a change in crystal structure. The volume of $Fe[HB(pz)_3]_2$ increases by 10% at the phase transition as indicated by volume expansion measurements. This parallels the 10.5% increase found in the Fe–N bond distance in $Fe[HB(pz)_3]_2$ as compared with the $Fe[HB(3,5\text{-}(CH_3)_2pz)_3]_2$ bond distance. As mentioned previously the shattering of the crystals of $Fe[H(pz)_3]_2$ can be easily observed upon heating them on a melting-point stage. The grinding of a freshly sublimed sample of $Fe[HB(pz)_3]_2$ reduced the temperature of the endotherm, and hence of the structural phase transition, from 432 K to as low as 409 K and also reduced the size of the endotherm. A similar effect may be observed if $Fe[HB(pz)_3]_2$ is diluted with zinc.[42] Apparently grinding reduces the "cooperative barrier" to the spin-state transition and the associated phase transition.

A comparison of the temperature of the structural phase transition as revealed by the DSC curve with the other indications of the spin state and structural transition seems to indicate rather different temperature ranges for the phase transition. However, it must be recalled that these results are obtained under quite different conditions. For instance, the Mössbauer spectra are obtained under a vacuum of ca. 1×10^{-4} Torr whereas the DSC results were obtained under helium at atmospheric pressure. Probably more important, the DSC was obtained at a constant heating rate of 10 K/min or over a period of ca. 15 min. In contrast, the Mössbauer spectra between 300 and 430 K were obtained over a period of several days during which the sample temperature was held constant for up to several hours during the measurement of an individual spectrum.

Acknowledgment. We thank Drs. T. E. Cranshaw and G. Longworth and L. W. Becker for many helpful discussions during the course of this work and J. Cloes for technical assistance. G.J.L. thanks the donors of the Petroleum Research Fund, administered by the American Chemical Society, for their support of this work and NATO for a cooperative scientific research grant (86/685). B.B.H. acknowledges the support of the Robert A. Welch Foundation through Grant No. B-483 and the Abilene Christian University Research Council.

Supplementary Material Available: Table I (magnetic susceptibility results for $Fe[HB(pz)_3]_2$), Table III (Mössbauer effect hyperfine parameters), Figure 4A (Mössbauer spectra of $Fe[HB(pz)_3]_2$ obtained between 300 and 400 K fit with two quadrupole doublets), and Figure 5A (Mössbauer spectra of $Fe[HB(pz)_3]_2$ obtained between 405 and 430 K fit with two quadrupole doublets) (6 pages). Ordering information is given on any current masthead page.

(42) Hutchinson, B. B. Unpublished results.

Notes

Contribution from the Department of Chemistry, University of Oregon, Eugene, Oregon 97403, and Jet Propulsion Laboratory, California Institute of Technology, Pasadena, California 91109

Photochemical Reactions of $Cp'_2Mo_2(CO)_6$ ($Cp' = \eta^5\text{-}C_5H_4CH_3$) with Amines. Descriptive Chemistry of the Disproportionation Reactions

Cecelia E. Philbin,[1] Albert E. Stiegman,[2] Steve C. Tenhaeff,[1] and David R. Tyler*[,1]

Received April 5, 1989

Irradiation of $Cp_2Mo_2(CO)_6$ in the presence of various phosphines and phosphite ligands leads to disproportionation of the metal–metal-bonded dimer:[3,4]

$$Cp_2Mo_2(CO)_6 + L \xrightarrow{h\nu} CpMo(CO)_3^- + CpMo(CO)_3L^+ \quad (1)$$
$$L = PR_3, P(OR)_3$$

Some time ago, Cox and co-workers[5] reported that irradiation of $Cp_2Mo_2(CO)_6$ in the presence of pyridine resulted in the formation of the $CpMo(CO)_3^-$ complex. It seemed likely that a disproportionation reaction analogous to that with phosphines and phosphites was occurring, but interestingly, no cationic carbonyl-containing product was spectroscopically identified in the reaction solution. We therefore decided to investigate in more detail the photochemical reactions of $Cp_2Mo_2(CO)_6$ with various amine ligands. Our emphasis was on determining if disproportionation was occurring, and if so, what the cationic product was. Herein we report that some amine ligands do disproportionate the $Cp'_2Mo_2(CO)_6$ dimer ($Cp' = \eta^5\text{-}C_5H_4CH_3$).[6] In those cases where disproportionation occurs, the products observed are dependent on the secondary reactions of the cationic product with the amine.

Experimental Section

All reactions of air-sensitive materials were performed under a nitrogen atmosphere by employing standard Schlenk techniques. $Cp'_2Mo_2(CO)_6$,[6,7] $[Cp'Mo(CO)_3py][BPh_4]$,[8] and $Mo(CO)_3(py)_3$[9] were synthesized according to literature procedures. Except where noted, all solvents were reagent grade. Pyridine (py) and triethylamine (NEt_3) were dried over the appropriate drying agent and distilled under nitrogen.[10] Cyclohexylamine (NH_2(c-Hx); c-Hx = cyclohexyl) and aniline were dried over the appropriate drying agent and vacuum-distilled.[10] Ethylenediamine

(1) University of Oregon.
(2) Jet Propulsion Laboratory.
(3) Stiegman, A. E.; Stieglitz, M.; Tyler, D. R. *J. Am. Chem. Soc.* **1983**, *105*, 6032–6037.
(4) Philbin, C. E.; Goldman, A. S.; Tyler, D. R. *Inorg. Chem.* **1986**, *25*, 4434–4436.
(5) Allen, D. M.; Cox, A.; Kemp, T. J.; Sultana, Q.; Pitts, R. B. *J. Chem. Soc., Dalton Trans.* **1976**, 1189–1193.
(6) $(\eta^5\text{-}CH_3C_5H_4)_2Mo_2(CO)_6$ was used instead of $(\eta^5\text{-}C_5H_5)_2Mo_2(CO)_6$ because the former complex is more soluble in the solvents employed in this study.
(7) Birdwhistle, R.; Hackett, P.; Manning, A. R. *J. Organomet. Chem.* **1978**, *157*, 239–241.
(8) Burkett-St. Laurent, C. T. R.; Field, J. S.; Haines, R. J.; McMahon, M. *J. Organomet. Chem.* **1979**, *181*, 117–130.
(9) Hieber, W.; Muhlbauer, F. *Z. Anorg. Allg. Chem.* **1935**, *221*, 337–339.
(10) Perrin, D. D.; Armarego, W. L.; Perrin, D. R. *Purification of Laboratory Chemicals*; Pergamon: Oxford, U.K., 1966.

0020-1669/89/1328-4414$01.50/0